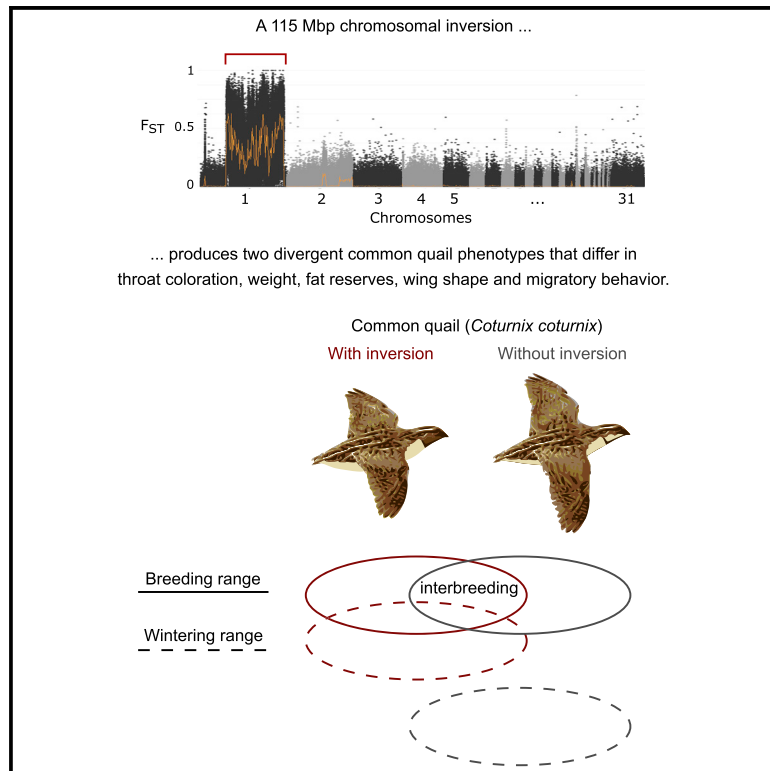


Massive genome inversion drives coexistence of divergent morphs in common quails

Graphical abstract



Authors

Ines Sanchez-Donoso, Sara Ravagni, J. Domingo Rodríguez-Teijeiro, ..., Matthew T. Webster, Jennifer A. Leonard, Carles Vilà

Correspondence

ines.sanchezdonoso@gmail.com (I.S.-D.), carles.vila@ebd.csic.es (C.V.)

In brief

Despite the extremely high mobility of common quail *Coturnix coturnix*, Sanchez-Donoso et al. identify a geographically restricted, very large chromosomal inversion in the darker, heavier common quail of the western edge of the species distribution. This inversion is also associated with reduced dispersal and migration.

Highlights

- A chromosomal inversion of 115 Mbp, 12% of the genome, is found in common quails
- Birds with the inversion are darker, heavier, and have rounder wings
- These birds do not undertake the characteristic long-distance migration
- The sequence in the inversion is highly divergent and originated before speciation



Report

Massive genome inversion drives coexistence of divergent morphs in common quails

Ines Sanchez-Donoso,^{1,8,9,*} Sara Ravagni,^{1,8} J. Domingo Rodríguez-Teijeiro,² Matthew J. Christmas,³ Yan Huang,⁴ Andros Maldonado-Linares,⁴ Manel Puigcerver,² Irene Jiménez-Blasco,² Pedro Andrade,^{5,6} David Gonçalves,^{5,6,7} Guillermo Friis,⁸ Ignasi Roig,⁴ Matthew T. Webster,³ Jennifer A. Leonard,^{1,8} and Carles Vilà^{1,8,*}

¹Conservation and Evolutionary Genetics Group, Estación Biológica de Doñana (EBD-CSIC), Seville 41092, Spain

²Departament de Biologia Evolutiva, Ecologia i Ciències Ambientals, Universitat de Barcelona, Barcelona 08028, Spain

³Department of Medical Biochemistry and Microbiology, Uppsala University, Uppsala 75123, Sweden

⁴Genome Integrity and Instability Group, Institut de Biotecnologia i Biomedicina, Departament de Biologia Cel·lular, Fisiologia i Immunologia, Universitat Autònoma de Barcelona, Cerdanyola del Vallès 08193, Spain

⁵CIBIO, Centro de Investigação em Biodiversidade e Recursos Genéticos, InBIO Laboratório Associado, Universidade do Porto, Vairão 4485-661, Portugal

⁶BIOPOLIS Program in Genomics, Biodiversity and Land Planning, CIBIO, Campus de Vairão, 4485-661 Vairão, Portugal

⁷Departamento de Biologia, Faculdade de Ciências, Universidade do Porto, Porto 4169-007, Portugal

⁸Center for Genomics and Systems Biology, New York University-Abu Dhabi, Abu Dhabi, United Arab Emirates

⁹Twitter: @consevol

^{*}Lead contact

^{*}Correspondence: ines.sanchezdonoso@gmail.com (I.S.-D.), carles.vila@ebd.csic.es (C.V.)

<https://doi.org/10.1016/j.cub.2021.11.019>

SUMMARY

The presence of population-specific phenotypes often reflects local adaptation or barriers to gene flow. The co-occurrence of phenotypic polymorphisms that are restricted within the range of a highly mobile species is more difficult to explain. An example of such polymorphisms is in the common quail *Coturnix coturnix*, a small migratory bird that moves widely during the breeding season in search of new mating opportunities, following ephemeral habitats,^{1,2} and whose females may lay successive clutches at different locations while migrating.³ In spite of this vagility, previous studies reported a higher frequency of heavier males with darker throat coloration in the southwest of the distribution (I. Jiménez-Blasco et al., 2015, Int. Union Game Biol., conference). We used population genomics and cytogenetics to explore the basis of this polymorphism and discovered a large inversion in the genome of the common quail. This inversion extends 115 Mbp in length and encompasses more than 7,000 genes (about 12% of the genome), producing two very different forms. Birds with the inversion are larger, have darker throat coloration and rounder wings, are inferred to have poorer flight efficiency, and are geographically restricted despite the high mobility of the species. Stable isotope analyses confirmed that birds carrying the inversion have shorter migratory distances or do not migrate. However, we found no evidence of pre- or post-zygotic isolation, indicating the two forms commonly interbreed and that the polymorphism remains locally restricted because of the effect on behavior. This illustrates a genomic mechanism underlying maintenance of geographically structured polymorphisms despite interbreeding with a lineage with high mobility.

RESULTS AND DISCUSSION

To assess the genetic structure of common quails that differ in phenotype in the western limit of the distribution (Figures 1A and S1), we sampled 80 male quails from Italy, Spain, Portugal, Morocco, and the eastern Atlantic archipelagos of Canary Islands and Madeira, including localities where different color morphs were dominant. We characterized genome-wide variation across these individuals using a reduced representation approach (supplemental information) and identified a large block of SNPs along chromosome 1 that was associated with very high differentiation (F_{ST}) between localities (Figure 1B). We assessed genetic structure for this region of chromosome 1 by using ADMIXTURE assuming 2 clusters. While the genetic

composition of many quails had 100% assignment to one cluster or the other, 30 had ~50:50 assignment to each cluster (Figure 1C), suggesting the existence of two chromosomal types. A principal-component analysis (PCA) of this region of chromosome 1 revealed well-defined groups of genotypes (Figure 1D), although this pattern was not observed when analyzing the rest of the genome (Figure S2). Homozygotes for one type, AA, constituted a cohesive group in the PCA (Figure 1D) and were widely distributed (Figure 1E). Homozygotes for the other type, BB, represented the other extreme of the variation in the PCA and were found only in the south of the Iberian Peninsula, Morocco, and the Atlantic islands. Heterozygotes, AB, were present in the same areas as BB. This shows that there is geographic structure in this species despite very high vagility^{1,2}



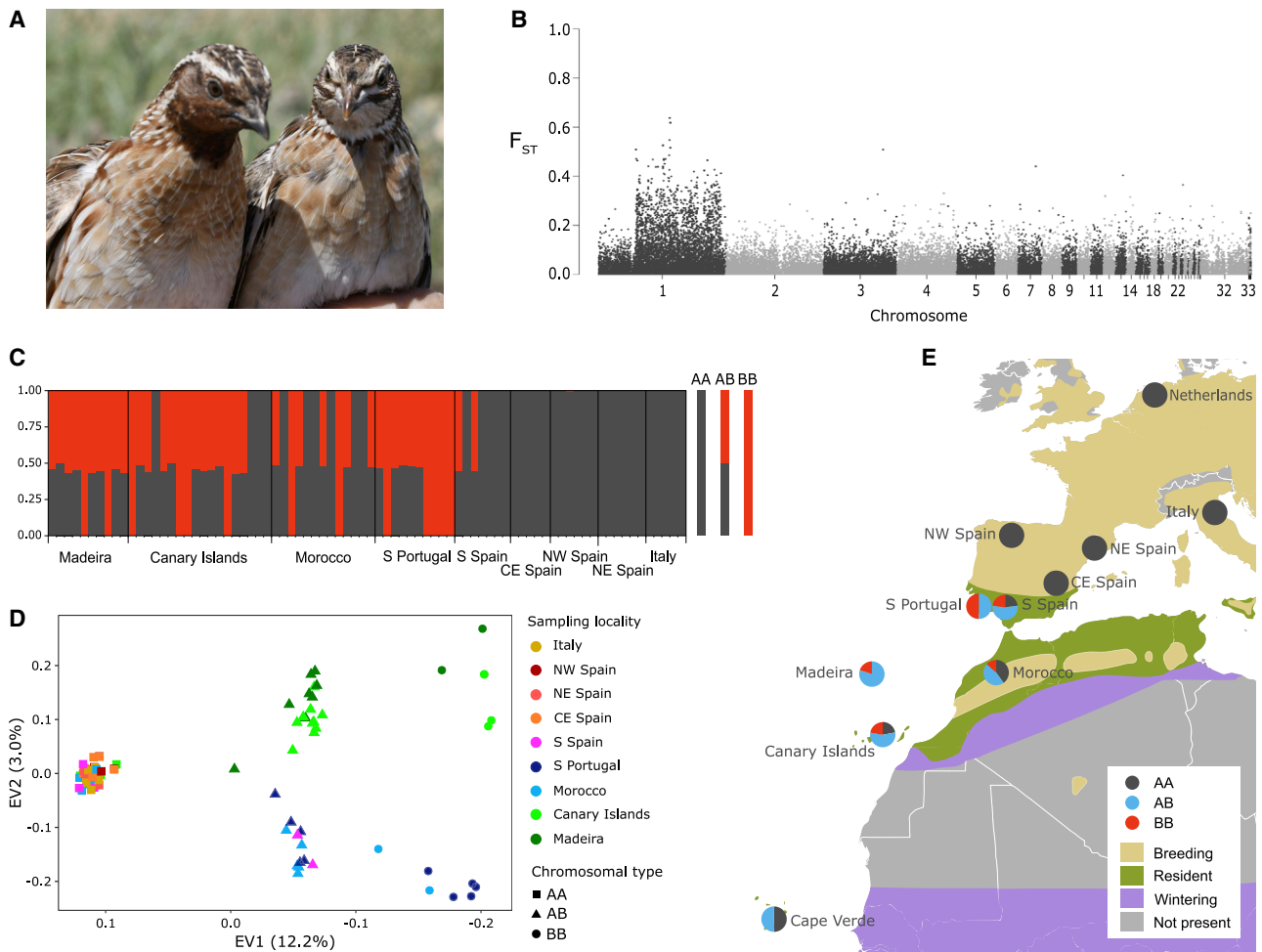


Figure 1. Genetic basis of phenotypic diversity in common quail

(A) Two common quail males captured in the same location in S Spain.

(B) F_{ST} for 60,024 SNPs along the genome quantifying differentiation across 80 male quails from 9 populations. Very large differentiation is observed in a large portion of chromosome 1.

(C) ADMIXTURE results (for $K = 2$) using 8,202 SNPs from the region with the largest F_{ST} differentiation in chromosome 1. For each individual, the analysis shows the proportion of the genome that belongs to each group. This allows the identification of three groups of individuals: AA, AB, and BB.

(D) Principal-component analysis (PCA) using the SNPs from the region with the largest F_{ST} differentiation in chromosome 1. AB and BB quails separate in clusters (mainland and island quails appear differentiated) while AA individuals cluster together independently of the locality of origin. For a PCA using SNPs outside the region, see [Figure S2](#).

(E) Distribution of genomic groups from a more complete survey of 119 male quails (gray, AA; blue, AB; red, BB).

For pigmentation of quails in each population, see [Figure S1](#). Figure related to [Data S1A](#).

and raises the question of how two distinct chromosomal forms can be maintained despite interbreeding.

The high F_{ST} over a large portion of chromosome 1 ([Figure 1B](#)) and the presence of three distinct putative genotypes could be explained by a chromosomal inversion that suppresses recombination in the region and favors the accumulation of differences between two haplotypes. To investigate the presence of an inversion, we captured six reproductively active males from northeastern Spain, where all previously sampled individuals belonged to type AA, and nine from southwestern Portugal, where individuals AB and BB had been identified. We synthesized probes for fluorescence *in situ* hybridization (FISH) assays. One of the probes was designed to hybridize to a DNA sequence inside the divergent region of chromosome

1, and the other one was outside this region. FISH assays on spermatocytes in meiotic prophase revealed that, in AA birds, the two probes in the paired chromatids were separated by a distance of $23.80 \mu\text{m}$ ($\text{SD} = \pm 4.25$; $n = 6$; [Table S1](#)). On the other hand, the samples from southern Portugal presented two patterns. BB quails had the two probes located at a smaller distance ($11.97 \mu\text{m} \pm 1.45$; $n = 5$), confirming that the probes were located on a different location along the chromosome, as expected if a large chromosomal inversion had taken place ([Figure 2](#)). In the remaining four AB birds, three fluorescent signals were identified, two of them corresponding to the probe located inside the divergent region, indicating that these individuals were heterokaryotypes (carrying one chromosome of each type) and that the two homologous

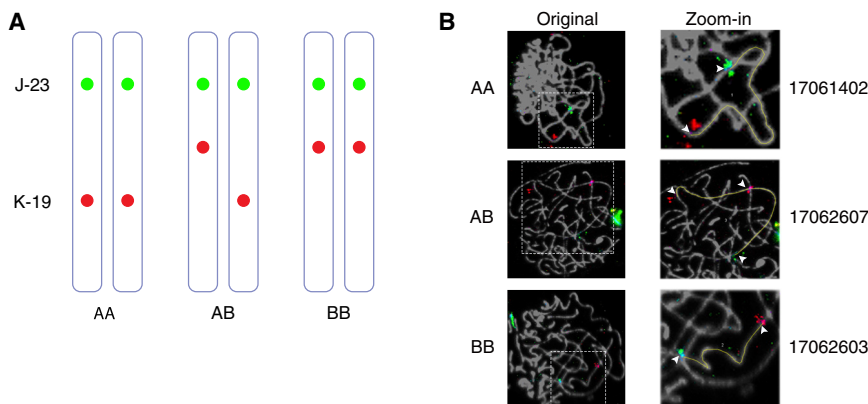


Figure 2. Immunofluorescence evidence of a chromosomal inversion

FISH assays using two probes for chromosome 1 in common quails, with one of the probes (K-19, red) located inside a region of the chromosome that could have suffered an inversion.

(A) Schematic representation of the three patterns observed, showing the position of the probes in AA, AB, and BB quails.

(B) Chromosomes during meiosis showing the position of J-23 (green probe, outside the inversion) and K-19 (red, inside the inversion) in three quails representing the three karyotypes.

See also [Table S1](#).

chromosomes were not completely paired during meiosis. These results confirm the presence of a large inversion in chromosome 1 and the presence of heterokaryotype quails in southern Portugal.

To better characterize the chromosomal limits of the inversion, we sequenced the complete genomes of 16 homokaryotype males at a coverage of $8.2\times$ – $13.5\times$ ([Table S2](#)). To simplify mapping and analyses, we avoided sequencing heterokaryotypes. We sequenced 10 BB homokaryotypes and 6 AA homokaryotypes from across the study area. This revealed 17,836,922 SNPs distributed along the genome. Genome-wide F_{ST} between the two groups, measured in 1-Kbp sliding windows, supported the presence of the inversion on chromosome 1, which extends 115 Mbp in length ([Figures 3A and S3](#)). This represents more than 12% of the genome and about $\frac{2}{3}$ of the largest chromosome in common quail. This inversion encompasses about 7,700 putative genes, whose alleles are in linkage disequilibrium due to substantially reduced recombination between inversion types ([Figure S4](#)). This results in a very large supergene,⁴ a chromosomal region encompassing multiple genes that are inherited together because of their genetic linkage. However, average F_{ST} along the inversion in longer windows (1 Mbp) showed that the differentiation between the lineages is higher near the limits of the inversion, implying some level of recombination between haplotypes inside the inverted region.⁵

The mean individual heterozygosity in the inverted region for BB quails was much lower than for AA quails, whereas outside the inverted region, heterozygosity was similar ([Figure 3B](#)). Measures of absolute divergence (d_{xy}) based on only the first and last 2 Mbp of the inversion (regions likely most resistant to recombination) were high ($d_{xy} = 0.0079$). Using a range of mutation rates estimated for birds, we calculated average divergences of 0.9–3.2 mya, but these are rough estimates because the sequences are not likely to be neutral. Of the 23,269 sites that were fixed differences between the inverted and non-inverted haplotypes in common quail chromosomes, the proportion of sites with the same allele as the Japanese quail assembly was 10.6 times higher for A haplotype than for B haplotype. This shows that the B haplotype was more divergent, indicating an old origin. Two alternative evolutionary histories could explain this observation. First, the divergent sequence of B haplotype could represent an old ancestral polymorphism, dating from before the divergence of Japanese and common quails and maintained

through incomplete lineage sorting. At the same time, the very limited diversity within the inverted region ([Figure 3B](#)) suggests that it has not accumulated many mutations compared to other parts of the genome. This could be the result of strong selective pressures reducing diversity due to hitchhiking or a low effective population size stemming from its limited distribution. Alternatively, the divergent sequence of B could derive from the more recent introgression of an inverted sequence originating in a separate species that likely diverged more than 1 mya. No other extant quail species that could be the source for this sequence inhabits the region where the inversion is found (Atlantic coast of SW Europe and NW Africa),⁶ but several extinct species of quail have been described for the eastern Atlantic islands,⁷ and one of these could have been the origin of the inversion. A similarly large inversion in white-throated sparrows, *Zonotrichia albicollis*, has been suggested to derive from introgression from a related species.⁸

The geographically limited distribution of the inversion is surprising given the high mobility of the species. After excluding the inverted region, analysis with ADMIXTURE of the genotype data obtained from the 16 complete genomes and from the reduced genomic representation approach of 80 quails failed to show any population differentiation between quails with and without the inversion (cross-validation suggested $K = 1$ clusters of genotypes), and a neighbor-joining tree of the sequences outside the inversion did not show any structure ([Figure 3C](#)). Similarly, the PCA with genomic data of the 80 quails, after excluding SNPs within the inversion ([Figure S2](#)), failed to show any grouping of samples corresponding to locality or genotype. These results imply frequent admixture and gene flow between quails with and without the inversion, confirming the absence of complete reproductive isolation and extensive gene flow across the western Palearctic, as suggested by the ringing data.⁹

We next investigated correlations between phenotype and karyotype. We used a subset of SNP markers to assess chromosomal composition of a larger sample of sexually active male quails from different locations and compiled morphological data. The three karyotype groups of quails differed in weight, with AA quails being the lightest (AA: mean \pm SD = 94.8 g \pm 6.9, $n = 43$; AB: 97.3 \pm 6.8, $n = 42$; BB: 99.8 \pm 6.4, $n = 18$; $F_{2,100} = 3.73$; $p = 0.027$; [Figure 4A](#); see [supplemental information](#)). They also showed significant differences in pigmentation: BB quails had darker throat coloration, while it was intermediate

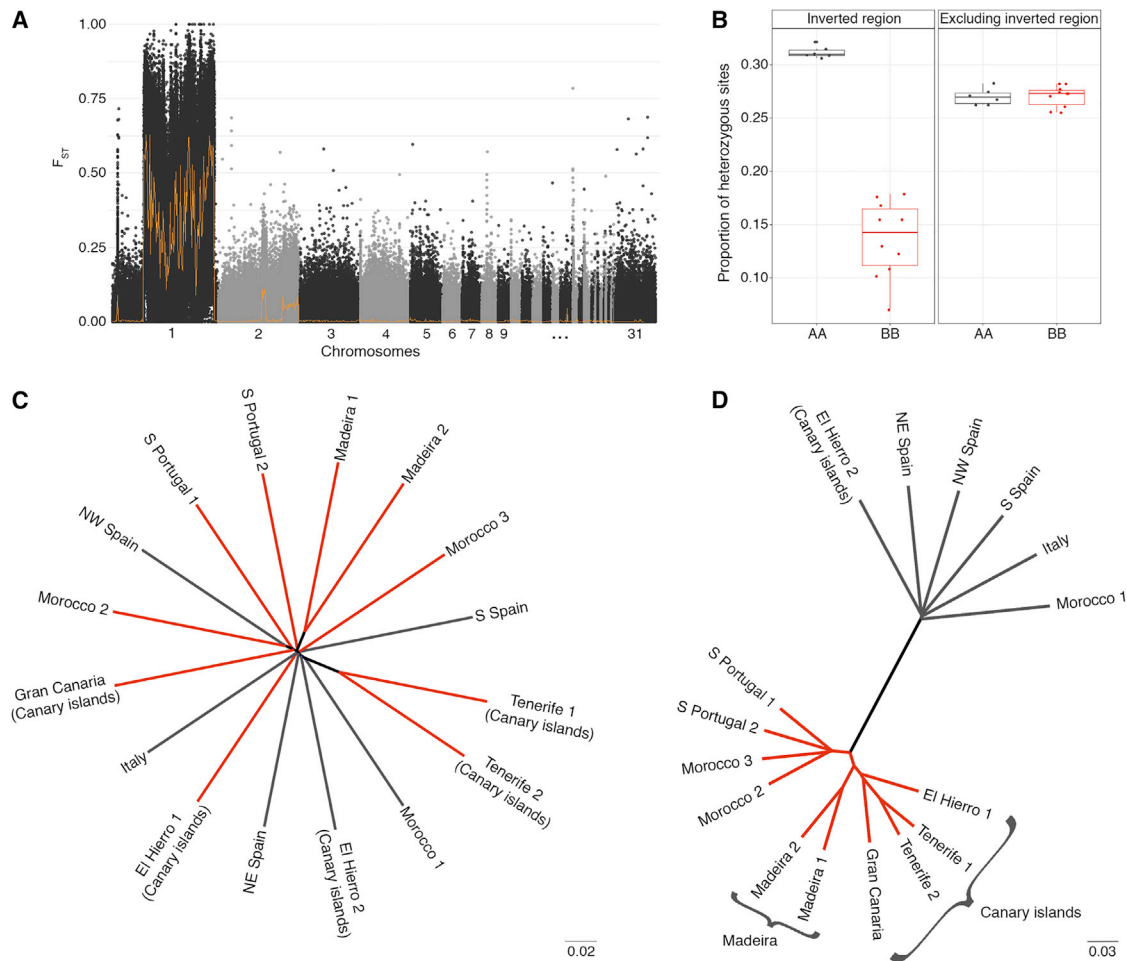


Figure 3. Genomic characterization of the inverted region in chromosome 1

(A) F_{ST} in 1-Kbp windows comparing homokaryotype AA ($n = 6$) and BB ($n = 10$) quails. A large portion of chromosome 1 shows extreme differentiation due to an inversion. The orange line represents F_{ST} values in 1-Mbp windows.

(B) Individual heterozygosity in homokaryotypes. Heterozygosity in the inverted region (left) is very much lower for BB quails, while it is similar between the two groups when excluding the inverted region (right).

(C) Neighbor-joining tree based on SNPs outside the inversion. AA in black and BB in red. Almost no geographic structure is observed.

(D) Tree based on SNPs within the inversion. Two large clusters appear separating the two groups of homokaryotypes. Additional clusters appear among BB quails, while AA individuals do not show any population structure.

See also [Figures S3](#) and [S4](#) and [Table S2](#).

for AB ([Figures 4B](#) and [S5](#); median color category for BB was 5, 4 for AB, and 2 for AA; $H(2) = 50.96$; $p < 0.001$). Interestingly, the genes RAB-38 and TYR, which have previously been found to affect pigmentation in birds,^{10,11} are very close to the inversion breakpoint and the genome sequences for AA and BB quails differ by several nonsynonymous substitutions in these genes ([Table S3](#)), suggesting that they could be associated with differences in pigmentation in this system too.

We also observed differences in the width of the pectoral lipid band as viewed through the skin, which is positively related to motor restlessness.¹² This band was significantly wider for AA quails than for AB and BB quails (AA: $6.58 \text{ mm} \pm 3.58$, $n = 43$; AB: 2.98 ± 2.05 , $n = 42$; BB: 2.44 ± 1.87 , $n = 18$; $F_{2,100} = 23.32$; $p < 0.001$; [Figure 4C](#)). We used wing measurements to calculate a modified Holynski index¹³ for each individual. Higher values for this index indicate that the wings are relatively narrower and

pointier, which is expected to indicate higher flight efficiency.¹⁴ The comparison of this index among the three karyotypes showed that AA quails had significantly higher values, while BB had lower values and AB had intermediate values (AA: 116.0 ± 10.6 , $n = 21$; AB: 104.9 ± 8.2 , $n = 38$; BB: 98.4 ± 11.0 , $n = 16$; $F_{2,72} = 16.78$; $p < 0.001$; [Figure 4D](#)), suggesting that the quails without the inversion (AA) had a more efficient flight apparatus. The limited flight efficiency of the quails with the inversion (AB and BB) could be associated with lack of or reduced migration. These phenotype patterns were not just an effect of latitudinal differences. Excluding AA quails from northern latitudes in the analyses gave the same results because AA quails did not differ in northern and southern localities ([Figure S6](#)).

To study the migratory behavior, we analyzed the isotopic signature of primary feathers from captured individuals. The isotopic signature for carbon ($\delta^{13}\text{C}$) and deuterium ($\delta^2\text{H}$) of feathers

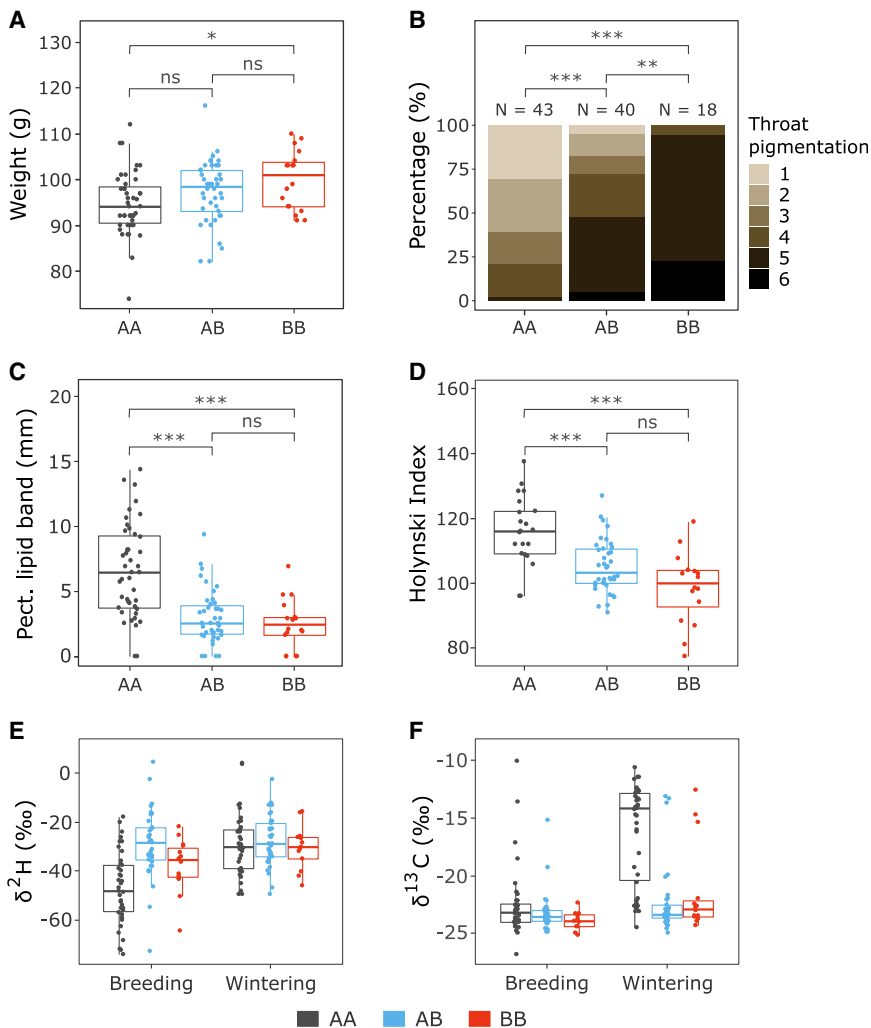


Figure 4. Morphology and isotopic signature in relation to the inversion

(A) Body weight of AA, AB, and BB male common quails.

(B) Proportion of individuals with different degrees of throat pigmentation.

(C) Width of the pectoral lipid band.

(D) Variation in the Holynski index, which measures wing pointedness and is related to flight efficiency. These morphological differences are not associated to latitude; see [Figure S6](#).

(E and F) Proportion of deuterium $\delta^2\text{H}$ (E) and carbon $\delta^{13}\text{C}$ isotopes (F) in two primary feathers from 1-year-old males, one grown during the previous breeding season and the other during the wintering season. AB and BB quails show small differences in the isotopic signature when comparing the two feathers, suggesting very reduced migratory movements compared to AA birds.

*** $p \leq 0.001$; ** $p \leq 0.01$; * $p \leq 0.05$; ns, non-significant. Figure related to [Data S1A](#) and [S1B](#).

Peninsula plus Morocco ([Figure 3D](#); see also [Figure 1D](#)). This suggests reduced mobility for quails carrying B haplotypes that results in population structure. On the other hand, A haplotypes did not show population differentiation. At the same time, sequences outside the inversion do not show any population structure ([Figures 3C](#) and [S2](#)). These results imply that quails with and without the inversion can freely interbreed, and their genomes recombine over most of their length. However, those that carry one or two copies of the inversion (AB and BB) have reduced mobility, leading to

is greatly determined by the frequency of these isotopes at the location where they were formed.¹⁵ We used feather wear and molting patterns to identify the age of quails. From 83 1-year-old males (Euring 5, the majority of the captured individuals), we took one primary feather that had been grown during the previous breeding season. This feather informed about the isotopic signature at the place of hatching. A second feather, grown in the wintering ground, allowed the comparison of the two locations. For the two isotopes, AA quails showed large differences between feathers grown in breeding and wintering grounds, while individuals that carried the inversion, either as homokaryotype BB or as heterokaryotype AB, showed very small differences ([Figures 4E](#) and [4F](#); [supplemental information](#)). This indicates that AB and BB birds did not migrate or that their migratory movements were much reduced as compared to quails without the inversion.

Reduced dispersal associated with the inverted sequence is further supported by a neighbor-joining tree representing the evolutionary relationships between the 16 genomes considering only the region within the inversion. The 10 BB quails sequenced formed groups corresponding to different geographic origins: Madeira, Canary Islands, and Iberian

population structure for the inverted sequence among geographic regions.

Chromosomal inversions are known to play an important role in evolution^{16,17} and can facilitate the coexistence of well-differentiated morphologies and behaviors,^{18,19} including differences in migration patterns.²⁰ In the case of the common quail, we have demonstrated that an inversion is associated with the coexistence of two complex sets of traits over part of the distribution range. The inversion is exceptionally large,¹⁷ resulting in a supergene that represents a considerable portion of the quail genome, more than 12%. Several quail species inhabited the Macaronesian archipelagos and went extinct during the Late Holocene as a result of human impacts. Some of these species had larger body sizes and reduced flying capacities⁷ and could have been the source of the inversion. The introgression of genes from a related species can facilitate adaptation,^{16,21,22} as in the case of the white-throated sparrow,⁸ where the introgression of an inversion has led to the coexistence of morphological and behavioral phenotypes.²³ However, we cannot exclude the possibility that the inversion in quails represents an ancestral polymorphism.

The presence of a large number of heterokaryotypes (AB) implies the absence of complete pre-zygotic isolation between the

two chromosomal types. Moreover, the lack of population structure excluding the inversion suggests the absence of post-zygotic genetic incompatibilities.

The restricted distribution of the inversion implies that heterozygotes also have reduced dispersal capacity and inter-island dispersal may have been the result of sweepstakes dispersal events.²⁴ This has been rare enough to result in genetic differentiation for the inversion, between islands and the mainland and between archipelagos. Patterns of genomic differentiation between AA and BB quails tend to decrease toward the center of the inversion (Figures 3A and S4), probably caused by occasional non-homologous pairing, which could allow some transfer of genetic material between the two chromosomal variants by double crossover events or by gene conversion.⁵ These double crossovers are occasionally observed²⁵ and may have contributed to an increase in genetic diversity in the region of the inversion in AA quails (Figure 3B) compared to the rest of the genome.

We do not have evidence of differences in fitness between the two chromosomal types. However, the distribution of the darker-colored birds carrying the inversion is restricted to warmer areas, as expected under Gloger's rule.²⁶ This could be associated with camouflage capacity or higher resistance of melanized feathers against keratinolytic bacteria, particularly in humid environments.^{26,27} The habitats occupied by AB and BB quails at the southern limit of the breeding range may also offer suitable habitats for the species all year round, allowing permanent habitation. In fact, AB and BB individuals were found in areas where the common quail populations have been suggested to be resident (Figure 1E).²⁸ The reduced recombination associated with the inversion facilitates the divergence between genes in this chromosomal region. This generates sufficient opportunity for the accumulation of substitutions that could facilitate local adaptation or even incompatibilities that could facilitate speciation.²⁹ Alternatively, frequency-dependent or temporally fluctuating selection due to changes in land uses induced by humans or climate^{16,30} could lead to stable polymorphisms over thousands of years. However, we know too little on the population dynamics of the two chromosomal types to understand the mechanisms of coexistence.

STAR★METHODS

Detailed methods are provided in the online version of this paper and include the following:

- KEY RESOURCES TABLE
- RESOURCE AVAILABILITY
 - Lead contact
 - Materials availability
 - Data and code availability
- EXPERIMENTAL MODEL AND SUBJECT DETAILS
- METHOD DETAILS
 - Field sampling
 - Molecular genetics
 - Immunofluorescence assays
 - Stable isotope analyses
- QUANTIFICATION AND STATISTICAL ANALYSIS
 - Phenotypic data
 - Genomic data
 - Stable isotope data

SUPPLEMENTAL INFORMATION

Supplemental information can be found online at <https://doi.org/10.1016/j.cub.2021.11.019>.

ACKNOWLEDGMENTS

The authors thank all the people who helped with the fieldwork and especially Francesc Sardà-Palomera, Jorge Falagán, and Fernando Gavilán (Spain); Mohamed Maghnouj (Morocco); Jan Staal (the Netherlands); and Pierfrancesco Micheloni (Italy). Joan Navarro and Francisco Ramírez provided support for isotopic analyses. Irene Quintanilla, Anna Cornellas, Sarai López, and the Laboratories of Molecular Ecology (LEM-EBD) and Stable Isotopes (LIE-EBD) at the Doñana Biological Station (EBD-CSIC) helped with the laboratory work. Genome sequencing was performed by the SNP&SEQ Technology Platform in Uppsala. The facility is part of the National Genomics Infrastructure (NGI) Sweden and Science for Life Laboratory. The SNP&SEQ Platform is also supported by the Swedish Research Council and the Knut and Alice Wallenberg Foundation. Informatic facilities were provided by Doñana ICTS-RBD. Microproject (C.V.) was funded by Severo Ochoa award from the Spanish Government to EBD-CSIC; Spanish Government grants PID2019-108163GB-I00 (C.V. and J.D.R.-T.), BFU2016-80370-P, and PID2019-107082RB-I00 (I.R.); Spanish Government fellowship BES-2017-081291 (S.R.); China Scholarship Council fellowship (Y.H.); and Fundação para a Ciência e Tecnologia Research Fellowship PD/BD/114028/2015 (P.A.). Federación de Caza de Euskadi provided financial support for part of the field sampling.

AUTHOR CONTRIBUTIONS

C.V. and I.S.-D. conceived the research. J.D.R.-T., M.P., I.J.-B., I.S.-D., C.V., P.A., and D.G. led the fieldwork, including sampling and phenotypic data collection. I.S.-D. and J.A.L. led stable isotope and molecular genetic lab work. I.R., Y.H., A.M.-L., and S.R. carried out immunofluorescence assays. S.R., I.S.-D., M.J.C., M.T.W., G.F., J.A.L., and C.V. carried out molecular genetic data analyses. I.S.-D., I.J.-B., and J.D.R.-T. carried out phenotype analyses. C.V., I.S.-D., and S.R. wrote the first version of the manuscript. All authors discussed and commented on the manuscript.

DECLARATION OF INTERESTS

The authors declare no competing interests.

Received: June 28, 2021

Revised: August 25, 2021

Accepted: November 8, 2021

Published: November 29, 2021

REFERENCES

1. Rodríguez-Teijeiro, J.D., Puigcerver, M., and Gallego, S. (1992). Mating strategy in the European quail (*Coturnix c. coturnix*) revealed by male population density and sex ratio in Catalonia (Spain). *Gibier Faune Sauvage* 9, 377–386.
2. Rodríguez-Teijeiro, J.D., Sardà-Palomera, F., Nadal, J., Ferrer, X., Ponz, C., and Puigcerver, M. (2009). The effects of mowing and agricultural landscape management on population movements of the common quail. *J. Biogeogr.* 36, 1891–1898.
3. Puigcerver, M., Rodrigo-Rueda, F.J., Rodríguez-Teijeiro, J.D., and Gallego, S. (1997). On the second clutches in the common quail (*Coturnix coturnix*). *Gibier Faune Sauvage* 14, 617–622.
4. Schwander, T., Libbrecht, R., and Keller, L. (2014). Supergenes and complex phenotypes. *Curr. Biol.* 24, R288–R294.
5. Navarro, A., Betrán, E., Barbadilla, A., and Ruiz, A. (1997). Recombination and gene flux caused by gene conversion and crossing over in inversion heterokaryotypes. *Genetics* 146, 695–709.
6. Madge, S., and McGowan, P. (2002). *Pheasants, Partridges and Grouse* (Princeton University).

7. Rando, J.C., Alcover, J.A., Pieper, H., Olson, S.L., Hernández, C.N., and López-Jurado, L.F. (2020). Unforeseen diversity of quails (Galliformes: Phasianidae: *Coturnix*) in oceanic islands provided by the fossil record of Macaronesia. *Zool. J. Linn. Soc.* *188*, 1296–1317.
8. Tuttle, E.M., Bergland, A.O., Korody, M.L., Brewer, M.S., Newhouse, D.J., Minx, P., Stager, M., Betuel, A., Cheviron, Z.A., Warren, W.C., et al. (2016). Divergence and functional degradation of a sex chromosome-like supergene. *Curr. Biol.* *26*, 344–350.
9. Guyomarc'h, J.C., Combreau, O., Puigcerver, M., Fontoura, P.A., and Aebischer, N.J. (1998). *Coturnix coturnix* quail. *Birds of the Western Palearctic Update 2*, 27–46.
10. Abolins-Abols, M., Kornobis, E., Ribeca, P., Wakamatsu, K., Peterson, M.P., Ketterson, E.D., and Milá, B. (2018). Differential gene regulation underlies variation in melanic plumage coloration in the dark-eyed junco (*Junco hyemalis*). *Mol. Ecol.* *27*, 4501–4515.
11. Mastrangelo, S., Cendron, F., Sottile, G., Niero, G., Portolano, B., Biscarini, F., and Cassandro, M. (2020). Genome-wide analyses identifies known and new markers responsible of chicken plumage color. *Animals (Basel)* *10*, E493.
12. Saint-Jame, M. (1990). La reproduction chez la caille des blés (*Coturnix c. coturnix*); études expérimentales des cycles saisonniers et de la variabilité interindividuelle. PhD thesis (Université de Rennes I).
13. Fiedler, W. (2005). Ecomorphology of the external flight apparatus of blackcaps (*Sylvia atricapilla*) with different migration behavior. *Ann. N Y Acad. Sci.* *1046*, 253–263.
14. Mönkkönen, M. (1995). Do migrant birds have more pointed wings?: a comparative study. *Evol. Ecol.* *9*, 520–528.
15. Rubenstein, D.R., and Hobson, K.A. (2004). From birds to butterflies: animal movement patterns and stable isotopes. *Trends Ecol. Evol.* *19*, 256–263.
16. Kirkpatrick, M., and Barton, N. (2006). Chromosome inversions, local adaptation and speciation. *Genetics* *173*, 419–434.
17. Wellenreuther, M., and Bernatchez, L. (2018). Eco-evolutionary genomics of chromosomal inversions. *Trends Ecol. Evol.* *33*, 427–440.
18. Küpper, C., Stocks, M., Risse, J.E., Dos Remedios, N., Farrell, L.L., McRae, S.B., Morgan, T.C., Karlionova, N., Pinchuk, P., Verkuil, Y.I., et al. (2016). A supergene determines highly divergent male reproductive morphs in the ruff. *Nat. Genet.* *48*, 79–83.
19. Huang, Y.C., Dang, V.D., Chang, N.C., and Wang, J. (2018). Multiple large inversions and breakpoint rewiring of gene expression in the evolution of the fire ant social supergene. *Proc. Biol. Sci.* *285*, 20180221.
20. Kirubakaran, T.G., Grove, H., Kent, M.P., Sandve, S.R., Baranski, M., Nome, T., De Rosa, M.C., Righino, B., Johansen, T., Otterå, H., et al. (2016). Two adjacent inversions maintain genomic differentiation between migratory and stationary ecotypes of Atlantic cod. *Mol. Ecol.* *25*, 2130–2143.
21. Jay, P., Whibley, A., Frézal, L., Rodríguez de Cara, M.Á., Nowell, R.W., Mallet, J., Dasmahapatra, K.K., and Joron, M. (2018). Supergene evolution triggered by the introgression of a chromosomal inversion. *Curr. Biol.* *28*, 1839–1845.e3.
22. Christmas, M.J., Wallberg, A., Bunikis, I., Olsson, A., Wallerman, O., and Webster, M.T. (2019). Chromosomal inversions associated with environmental adaptation in honeybees. *Mol. Ecol.* *28*, 1358–1374.
23. Merritt, J.R., Grogan, K.E., Zinzow-Kramer, W.M., Sun, D., Ortlund, E.A., Yi, S.V., and Maney, D.L. (2020). A supergene-linked estrogen receptor drives alternative phenotypes in a polymorphic songbird. *Proc. Natl. Acad. Sci. USA* *117*, 21673–21680.
24. de Queiroz, A. (2005). The resurrection of oceanic dispersal in historical biogeography. *Trends Ecol. Evol.* *20*, 68–73.
25. Stevison, L.S., Hoehn, K.B., and Noor, M.A.F. (2011). Effects of inversions on within- and between-species recombination and divergence. *Genome Biol. Evol.* *3*, 830–841.
26. Delhey, K. (2019). A review of Gloger's rule, an ecogeographical rule of colour: definitions, interpretations and evidence. *Biol. Rev. Camb. Philos. Soc.* *94*, 1294–1316.
27. Burt, E.H., and Ichida, J.M. (2004). Gloger's rule, feather-degrading bacteria, and color variation among Song Sparrows. *Condor* *106*, 681–686.
28. BirdLife International (2021). Species factsheet: *Coturnix coturnix*. <https://www.birdlife.org>.
29. Faria, R., and Navarro, A. (2010). Chromosomal speciation revisited: rearranging theory with pieces of evidence. *Trends Ecol. Evol.* *25*, 660–669.
30. Lamichaney, S., Fan, G., Widemo, F., Gunnarsson, U., Thalmann, D.S., Hoepfner, M.P., Kerje, S., Gustafson, U., Shi, C., Zhang, H., et al. (2016). Structural genomic changes underlie alternative reproductive strategies in the ruff (*Philomachus pugnax*). *Nat. Genet.* *48*, 84–88.
31. Alexander, D.H., Novembre, J., and Lange, K. (2009). Fast model-based estimation of ancestry in unrelated individuals. *Genome Res.* *19*, 1655–1664.
32. Li, H., and Durbin, R. (2009). Fast and accurate short read alignment with Burrows-Wheeler transform. *Bioinformatics* *25*, 1754–1760.
33. Kopelman, N.M., Mayzel, J., Jakobsson, M., Rosenberg, N.A., and Mayrose, I. (2015). Clumpak: a program for identifying clustering modes and packaging population structure inferences across K. *Mol. Ecol. Resour.* *15*, 1179–1191.
34. Martin, M. (2011). Cutadapt removes adapter sequences from high-throughput sequencing reads. *EMBnet. J.* *17*, 10–12.
35. Lenth, R. (2020). emmeans: estimated marginal means, aka least-squares means. <https://cran.r-project.org/web/packages/emmeans/index.html>.
36. Andrews, S. (2010). FastQC: a quality control tool for high throughput sequence data. <https://www.bioinformatics.babraham.ac.uk/projects/fastqc/>.
37. Garrison, E., and Marth, G. (2012). Haplotype-based variant detection from short-read sequencing. *arXiv*, arXiv:1207.3907. <https://arxiv.org/abs/1207.3907>.
38. McKenna, A., Hanna, M., Banks, E., Sivachenko, A., Cibulskis, K., Kernysky, A., Garimella, K., Altshuler, D., Gabriel, S., Daly, M., and DePristo, M.A. (2010). The Genome Analysis Toolkit: a MapReduce framework for analyzing next-generation DNA sequencing data. *Genome Res.* *20*, 1297–1303.
39. Robinson, J.T., Thorvaldsdóttir, H., Winckler, W., Guttman, M., Lander, E.S., Getz, G., and Mesirov, J.P. (2011). Integrative genomics viewer. *Nat. Biotechnol.* *29*, 24–26.
40. Thorvaldsdóttir, H., Robinson, J.T., and Mesirov, J.P. (2013). Integrative Genomics Viewer (IGV): high-performance genomics data visualization and exploration. *Brief. Bioinform.* *14*, 178–192.
41. Rasband, W.S. (2018). ImageJ (US National Institutes of Health). <https://imagej.nih.gov/ij/>.
42. Shin, J.H., Blay, S., McNeney, B., and Graham, J. (2006). LDheatmap: an R function for graphical display of pairwise linkage disequilibrium between single nucleotide polymorphisms. *J. Stat. Softw.* *16*, 1–9.
43. Katoh, K., and Standley, D.M. (2013). MAFFT multiple sequence alignment software version 7: improvements in performance and usability. *Mol. Biol. Evol.* *30*, 772–780.
44. Purcell, S., Neale, B., Todd-Brown, K., Thomas, L., Ferreira, M.A., Bender, D., Maller, J., Sklar, P., de Bakker, P.I., Daly, M.J., and Sham, P.C. (2007). PLINK: a tool set for whole-genome association and population-based linkage analyses. *Am. J. Hum. Genet.* *81*, 559–575.
45. R Development Core Team (2020). R: A language and environment for statistical computing (R Foundation for Statistical Computing).
46. Wickham, H. (2009). ggplot2: Elegant Graphics for Data Analysis (Springer-Verlag). <https://ggplot2.tidyverse.org>.
47. Turner, S.D. (2018). qqman: an R package for visualizing GWAS results using Q-Q and manhattan plots. *J. Open Source Softw.* *3*, 731.

48. Zheng, X., Levine, D., Shen, J., Gogarten, S.M., Laurie, C., and Weir, B.S. (2012). A high-performance computing toolset for relatedness and principal component analysis of SNP data. *Bioinformatics* **28**, 3326–3328.
49. RStudio Team (2020). RStudio: integrated development for R (R Foundation for Statistical Computing).
50. Li, H., Handsaker, B., Wysoker, A., Fennell, T., Ruan, J., Homer, N., Marth, G., Abecasis, G., and Durbin, R.; 1000 Genome Project Data Processing Subgroup (2009). The sequence alignment/map format and SAMtools. *Bioinformatics* **25**, 2078–2079.
51. Cingolani, P., Platts, A., Wang, L., Coon, M., Nguyen, T., Wang, L., Land, S.J., Lu, X., and Ruden, D.M. (2012). A program for annotating and predicting the effects of single nucleotide polymorphisms, SnpEff: SNPs in the genome of *Drosophila melanogaster* strain w1118; iso-2; iso-3. *Fly (Austin)* **6**, 80–92.
52. Glaubitz, J.C., Casstevens, T.M., Lu, F., Harriman, J., Elshire, R.J., Sun, Q., and Buckler, E.S. (2014). TASSEL-GBS: a high capacity genotyping by sequencing analysis pipeline. *PLoS ONE* **9**, e90346.
53. Danecek, P., Auton, A., Abecasis, G., Albers, C.A., Banks, E., DePristo, M.A., Handsaker, R.E., Lunter, G., Marth, G.T., Sherry, S.T., et al.; 1000 Genomes Project Analysis Group (2011). The variant call format and VCFtools. *Bioinformatics* **27**, 2156–2158.
54. Mur, P. (1994). Contribution à la gestion des populations paléarctiques de caille des blés dans la phase européenne de son cycle annuel. Recherches méthodologiques sur la cinétique démographique et appréciation des facteurs de fluctuations. PhD thesis (University of Rennes I).
55. Rodríguez-Teijeiro, J.D., Barroso, A., Gallego, S., Puigcerver, M., and Vinyoles, D. (2006). Orientation-cage experiments with the European Quail during the breeding season and autumn migration. *Can. J. Zool.* **84**, 887–894.
56. Jenni, L., and Winkler, R. (1989). The feather-length of small passerines: a measurement for wing-length in live birds and museum skins. *Bird Study* **36**, 1–15.
57. Newton, I. (2010). *Bird Migration* (William Collins).
58. Saint Jalme, M., and Guyomarc'h, J.C. (1995). Plumage development and moult in the European Quail *Coturnix c. coturnix*: criteria for age determination. *Ibis* **137**, 570–581.
59. Elshire, R.J., Glaubitz, J.C., Sun, Q., Poland, J.A., Kawamoto, K., Buckler, E.S., and Mitchell, S.E. (2011). A robust, simple genotyping-by-sequencing (GBS) approach for high diversity species. *PLoS ONE* **6**, e19379.
60. Patterson, N., Price, A.L., and Reich, D. (2006). Population structure and eigenanalysis. *PLoS Genet.* **2**, e190.
61. Price, A.L., Patterson, N.J., Plenge, R.M., Weinblatt, M.E., Shadick, N.A., and Reich, D. (2006). Principal components analysis corrects for stratification in genome-wide association studies. *Nat. Genet.* **38**, 904–909.
62. Weir, B.S., and Cockerham, C.C. (1984). Estimating F-statistics for the analysis of population structure. *Evolution* **38**, 1358–1370.
63. Camacho-Sanchez, M., Quintanilla, I., Hawkins, M.T.R., Tuh, F.Y.Y., Wells, K., Maldonado, J.E., and Leonard, J.A. (2018). Interglacial refugia on tropical mountains: novel insights from the summit rat (*Rattus baluensis*), a Borneo mountain endemic. *Divers. Distrib.* **24**, 1252–1266.
64. Roig, I., Dowdle, J.A., Toth, A., de Rooij, D.G., Jasin, M., and Keeney, S. (2010). Mouse TRIP13/PCH2 is required for recombination and normal higher-order chromosome structure during meiosis. *PLoS Genet.* **6**, e1001062.
65. Pacheco, S., Marcet-Ortega, M., Lange, J., Jasin, M., Keeney, S., and Roig, I. (2015). The ATM signaling cascade promotes recombination-dependent pachytene arrest in mouse spermatocytes. *PLoS Genet.* **11**, e1005017.
66. Zlotina, A., Galkina, S., Krasikova, A., Crooijmans, R.P., Groenen, M.A., Gaginskaya, E., and Deryusheva, S. (2012). Centromere positions in chicken and Japanese quail chromosomes: de novo centromere formation versus pericentric inversions. *Chromosome Res.* **20**, 1017–1032.
67. Pacheco, S., Maldonado-Linares, A., Marcet-Ortega, M., Rojas, C., Martínez-Marchal, A., Fuentes-Lazaro, J., Lange, J., Jasin, M., Keeney, S., Fernández-Capetillo, O., et al. (2018). ATR is required to complete meiotic recombination in mice. *Nat. Commun.* **9**, 2622.
68. Wassenaar, L.I., and Hobson, K.A. (2003). Comparative equilibration and online technique for determination of non-exchangeable hydrogen of keratins for use in animal migration studies. *Isotopes Environ. Health Stud.* **39**, 211–217.
69. Holynski, R.B. (1965). The methods of analysis of wing-formula variability (English summary). *Notatki Orn.* **6**, 21–25.
70. Lockwood, R., Swaddle, J.P., and Rayner, J.M.V. (1998). Avian wingtip shape reconsidered: wingtip shape indices and morphological adaptations to migration. *J. Avian Biol.* **29**, 273–292.
71. Fox, J., and Weisberg, S. (2019). *An R Companion to Applied Regression*, Third Edition (Sage).
72. Puritz, J.B., Hollenbeck, C.M., and Gold, J.R. (2014). dDocent: a RADseq, variant-calling pipeline designed for population genomics of non-model organisms. *PeerJ* **2**, e431.
73. Bourgeois, Y.X.C., Bertrand, J.A., Delahaie, B., Cornuault, J., Duval, T., Milá, B., and Thébaud, C. (2016). Candidate gene analysis suggests untapped genetic complexity in melanin-based pigmentation in birds. *J. Hered.* **107**, 327–335.
74. El Sabry, M.I., Eshak, M.G., Stino, F.K.R., and Bondioli, K.R. (2017). Comparing growth, immune and pigmentation related gene expression in three lines of Japanese and wild European quail. *Anim. Sci. Pap. Rep.* **35**, 407–418.
75. Liu, X., Zhou, R., Peng, Y., Zhang, C., Li, L., Lu, C., and Li, X. (2019). Correction to: Hair follicles transcriptome profiles in Bashang long-tailed chickens with different plumage colors. *Genes Genomics* **41**, 1369.
76. Loftus, S.K., Larson, D.M., Baxter, L.L., Antonellis, A., Chen, Y., Wu, X., Jiang, Y., Bittner, M., Hammer, J.A., 3rd, and Pavan, W.J. (2002). Mutation of melanosome protein RAB38 in chocolate mice. *Proc. Natl. Acad. Sci. USA* **99**, 4471–4476.
77. Protas, M.E., and Patel, N.H. (2008). Evolution of coloration patterns. *Annu. Rev. Cell Dev. Biol.* **24**, 425–446.
78. Xi, Y., Liu, H., Li, L., Xu, Q., Liu, Y., Wang, L., Ma, S., Wang, J., Bai, L., Zhang, R., and Han, C. (2020). Transcriptome reveals multi pigmentation genes affecting dorsoventral pattern in avian body. *Front. Cell Dev. Biol.* **8**, 560766.
79. Bazzi, G., Podofillini, S., Gatti, E., Gianfranceschi, L., Cecere, J.G., Spina, F., Saino, N., and Rubolini, D. (2017). Candidate genes have sex-specific effects on timing of spring migration and moult speed in a long-distance migratory bird. *Curr. Zool.* **63**, 479–486.
80. Mettler, R., Segelbacher, G., and Schaefer, H.M. (2015). Interactions between a candidate gene for migration (ADCYAP1), morphology and sex predict spring arrival in blackcap populations. *PLoS ONE* **10**, e0144587.
81. Steinmeyer, C., Mueller, J.C., and Kempnaers, B. (2009). Search for informative polymorphisms in candidate genes: clock genes and circadian behaviour in blue tits. *Genetica* **136**, 109–117.
82. Nam, K., Mugal, C., Nabholz, B., Schielzeth, H., Wolf, J.B., Backström, N., Künstner, A., Balakrishnan, C.N., Heger, A., Ponting, C.P., et al. (2010). Molecular evolution of genes in avian genomes. *Genome Biol.* **11**, R68.
83. Smeds, L., Qvarnström, A., and Ellegren, H. (2016). Direct estimate of the rate of germline mutation in a bird. *Genome Res.* **26**, 1211–1218.
84. Puigcerver, M., Gallego, S., Rodríguez-Teijeiro, J.D., and Senar, J.C. (1992). Survival and mean life span of the quail *Coturnix c. coturnix*. *Bird Study* **39**, 120–123.

STAR★METHODS

KEY RESOURCES TABLE

| REAGENT or RESOURCE | SOURCE | IDENTIFIER |
|--|---|---|
| Antibodies | | |
| Primary antibody anti- rabbit SYCP3 | Abcam | 1:400, Abcam Cat# ab15093; RRID: AB_301639 |
| Goat anti-rabbit DyLight 649 | Jackson ImmunoResearch Lab | 1:400, Jackson ImmunoResearch Lab Cat# 108-495-003; RRID: AB_2337515 |
| Chemicals, peptides, and recombinant proteins | | |
| Restriction enzyme EcoT22I | N/A | N/A |
| Restriction enzyme Nsil | N/A | N/A |
| Axial core marker SYCP3 | Abcam | ab97672 |
| Digoxigenin-11-dUTP | Roche | 11093088910 |
| Biotin-16-dUTP | Roche | 11093070910 |
| Cot-1 DNA | Invitrogen | 18440016 |
| Salmon sperm DNA | Stratagene | 201190 |
| Alexa Fluor 555 streptavidin | Invitrogen | S-21381 |
| Anti-Digoxigenin-Fluorescein | Roche | 11207741910 |
| Critical commercial assays | | |
| DNeasy Blood & Tissue Kit | QIAGEN | Cat. No. / ID: 69506 |
| Deposited data | | |
| Genomic data | GenBank | GenBank: PRJNA730394 |
| Genotyping-by-sequencing data (non filtered SNPs) | CSIC Repository https://digital.csic.es/handle/10261/251279 | Doi: https://dx.doi.org/10.20350/digitalCSIC/13989 |
| Results of the FISH assays | This paper | Table S1 |
| Sample information and all morphological and stable isotope data | This paper | Data S1 |
| Software and algorithms | | |
| ACO XY Software | A.COLOMA Open microscopy | N/A |
| ADMIXTURE v1.3.0 | Alexander et al. ³¹ | https://bioinformaticshome.com/tools/descriptions/ADMIXTURE.html |
| Adobe Photoshop | Adobe | N/A |
| BWA-MEM v.0.7.15 and v.0.7.8-r455 | Li and Durbin ³² | https://github.com/lh3/bwa |
| CLUMPAK server | Kopelman et al. ³³ | http://clumpak.tau.ac.il/ |
| CUTADAPT v.1.17 | Martin ³⁴ | https://cutadapt.readthedocs.io/en/stable/ |
| Emmeans package | Lenth ³⁵ | https://cran.r-project.org/web/packages/emmeans/index.html |
| FASTQC v.0.11.5 | Andrews ³⁶ | https://www.bioinformatics.babraham.ac.uk/projects/fastqc/ |
| FREEBAYES v.1.3.1 | Garrison and Marth ³⁷ | https://arxiv.org/abs/1207.3907 |
| GATK v3.6 | McKenna et al. ³⁸ | https://gatk.broadinstitute.org/hc/en-us |
| IGV v.2.5.2 | Robinson et al. ³⁹ and Thorvaldsdóttir et al. ⁴⁰ | https://software.broadinstitute.org/software/igv/ |
| ImageJ | Rasband ⁴¹ | https://imagej.nih.gov/ij/download.html |
| LDHeatMap package | Shin et al. ⁴² | https://cran.r-project.org/web/packages/LDheatmap/index.html |
| MAFFT aligner | Katoh and Standley ⁴³ | https://mafft.cbrc.jp/alignment/server/ |
| Original script for dxy calculations | Matthew J. Christmas GitHub | https://github.com/MattChristmas/Quail_inversion_scripts |
| PICARD v.2.4.1 | Broad Institutet | https://broadinstitute.github.io/picard/ |

(Continued on next page)

Continued

| REAGENT or RESOURCE | SOURCE | IDENTIFIER |
|---|---------------------------------------|---|
| PLINK v1.90b6.10 | Purcell et al. ⁴⁴ | https://www.cog-genomics.org/plink/ |
| R 4.0.3 | R Development Core Team ⁴⁵ | https://cran.r-project.org/bin/windows/base/ |
| R package ggplot2 | Wickham ⁴⁶ | https://ggplot2.tidyverse.org |
| R package qqman | Turner ⁴⁷ | http://cran.nexr.com/web/packages/qqman/index.html |
| R package SNPRelate | Zheng et al. ⁴⁸ | https://www.bioconductor.org/packages/release/bioc/html/SNPRelate.html |
| RStudio v1.3.959 | RStudio Team ⁴⁹ | https://www.rstudio.com/ |
| SAMtools v. 1.6.0 | Li et al. ⁵⁰ | http://www.htslib.org/ |
| SnEff v.4.3t | Cingolani et al. ⁵¹ | http://pcingola.github.io/SnpEff/ |
| TASSEL-3-GBS pipeline | Glaubitz et al. ⁵² | https://bytebucket.org/tasseladmin/tassel-5-source/wiki/docs/TasselPipelineGBS.pdf |
| vcffilter | SASC team | https://github.com/vcflib/vcflib/blob/master/doc/vcffilter.md |
| VCFTOOLS v.0.1.13 | Danecek et al. ⁵³ | http://vcftools.sourceforge.net/ |
| Other | | |
| Japanese quail genome (<i>Coturnix japonica</i>) | RefSeq | RefSeq: GCF_001577835.1 |
| Japanese quail genome (<i>Coturnix japonica</i>) | GENBANK | GenBank: GCA_001577835.1 |
| Flash HT Plus elemental analyzer coupled to a Delta-V Advantage isotope ratio mass spectrometer via a CONFLO IV interface | Thermo Fisher Scientific | N/A |
| FISH probe K19 | NCBI | NCBI: WAG-22K19 |
| FISH probe J23 | NCBI | NCBI: WAG-22J23 |

RESOURCE AVAILABILITY

Lead contact

Further information and requests for resources and reagents should be directed to and will be fulfilled by the Lead Contact, Ines Sanchez-Donoso (ines.sanchezdonoso@gmail.com).

Materials availability

This study did not generate new materials.

Data and code availability

Genomic data are deposited in GenBank (GenBank: PRJNA730394). Genotyping-by-sequencing data (non filtered SNPs) are accessible in <https://digital.csic.es/handle/10261/251279> (<https://dx.doi.org/10.20350/digitalCSIC/13989>). Results of the FISH assays are included in Table S1 in this publication. Original script for *dxy* calculations is provided in https://github.com/MattChristmas/Quail_inversion_scripts. Any additional information required to reanalyze the data reported in this paper is available from the lead contact upon request.

EXPERIMENTAL MODEL AND SUBJECT DETAILS

The common quail is a Galliform with a wide distribution in the Palearctic region and in southern Africa. Eurasian populations winter in the Sahel and India,⁹ reaching breeding grounds in northern Africa and Eurasia between February and March. It is a highly mobile species that combines these trans-Saharan migratory movements with nomadic movements during the breeding season in search of suitable but ephemeral habitats of mainly winter cereal crops, such as wheat and barley.² As cereal maturation depends on latitude and altitude, destruction of this habitat due to harvesting forces quails to move in an asynchronous manner, following a “green wave.” After harvest, only females with broods remain in the breeding areas to raise their chicks.² Chicks remain with their mothers for about 4 weeks⁵⁴ and females can lay several clutches, at very different locations, during the breeding season.³ As sex ratio is unbalanced toward males, unpaired males move extensively during the breeding season in search of females.⁵⁵ The common quail is a popular game species in many countries in Western Europe and ring recoveries confirm that philopatry is small and

that quails move extensively across Western Europe¹. The population size of this species is estimated at 15–35 million individuals.²⁸

Sample information and all morphological and stable isotope data are included as supplemental datasets (Data S1A and S1B, respectively). Sampling and animal handling procedures conformed to relevant institutional and national guidelines and regulations in bioethics. All our experimental work was carried out in accordance with the ASAB/ABS Guidelines for the treatment of animals. Fieldwork in Spain and Morocco was conducted under the supervision of J.D. Rodríguez-Teijeiro and M. Puigcerver following the guidelines of the Federation of European Laboratory Animal Science Associations (FELASA), under sampling permits awarded by the regional governments. Portuguese samples were obtained under sampling permits 634/2017/CAPT and 635/2017/CAPT from ICNF (“Instituto da Conservação da Natureza e das Florestas”) to David Gonçalves and Pedro Andrade. Sampling permit for Madeira was granted by “Secretaria Regional do Ambiente e Recursos Naturais,” 8/PNM/2015-MAD. Cape Verde samples were obtained under sampling permit 08/2016 from “Ministério da Agricultura e Ambiente” to J.D. Rodríguez-Teijeiro. The work fulfilled the ethical recommendations of the European Union and the Spanish legislation (Spanish Law 5/1995 and Decree 214/1997) and was approved by the Ethics Committee on Animal Experimentation from the University of Barcelona.

METHOD DETAILS

Field sampling

We captured common quail males during the breeding season in Spain, Portugal, Morocco, Italy, Netherlands and the Atlantic archipelagos of Madeira, Canary Islands and Cape Verde (Data S1A). We collected phenotypic data from each captured quail. We weighed the captured quails with a precision scale to the nearest ± 0.5 g and measured the width of their pectoral lipid band (viewed through the skin) with a caliper (± 0.01 mm). We measured maximum folded wing length with a zero-stop ruler (± 0.5 mm) by flattening the camber and straightening the lateral curvature of the wing, and the length of each primary feather and the second secondary from one wing with a pin ruler (± 0.5 mm).⁵⁶

We also took pictures of the throat to study pigmentation. In common quails molt is split between the breeding area and the wintering area,⁵⁷ and some feathers are grown in each area. For each individual we inferred age from the patterns of molt and wear of the primaries⁵⁸ and took feather samples for isotope analyses. The feathers were chosen taking into account the age category, and we sampled one feather grown in the breeding area and another one grown in the wintering grounds. About 100 μ l of blood was extracted from each individual from the jugular vein for genomic analyses. After sampling, birds were released in the place of capture except for 15 individuals for which we sampled the testes for the immunofluorescence assays (Table S1). In this case, birds were immediately dissected and testicles were frozen in liquid nitrogen or dry ice.

Molecular genetics

Genotyping by sequencing

DNA was extracted by using the DNeasy Blood & Tissue Kit of QIAGEN. We genotyped quail samples using a reduced representation genotype-by-sequencing (GBS) approach, which consists of next generation sequencing short fragments of DNA (64 bp) starting at the cutting point of some restriction enzymes.⁵⁹ We built a shotgun library from DNA of 80 quails from 9 localities (plus a control) after digestion with the restriction enzyme EcoT22I. This library was sequenced using Illumina HiSeq 2500 (1x100bp) at Cornell University, Biotechnology Resource Center. We called SNPs using the TASSEL-3-GBS pipeline⁵² and mapped the obtained sequences against the Japanese quail genome (*Coturnix japonica*, RefSeq assembly accession number: GCF_001577835.1) using BWA-MEM v.0.7.8-r455.³² We filtered for biallelic SNPs with minor allele frequency higher than 0.03, missing data less than 25%, minimum quality of 20 and depth higher than 5 and lower than 100 using VCFTOOLS v.0.1.13.⁵³ After applying these filters, we retained 60,024 SNPs.

We assessed population structure with a principal component analysis (PCA) with the function `snpgdsPCA`^{60,61} in the R package SNPRelate.⁴⁸ To assess regions of the genome responsible for population differentiation, we calculated Weir and Cockerham's F_{ST} ⁶² among the 9 localities for each SNP along the genome estimator implemented in VCFTOOLS. We plotted F_{ST} values with the package `qqman`⁴⁷ in R 4.0.3,⁴⁵ using RStudio v1.3.959.⁴⁹

Analyses of population structure were carried out with ADMIXTURE v1.3.0.³¹ To determine the number of clusters (K) that best explain the data for different SNP datasets, we ran 20 independent analyses using the flag “K” from K = 1 to K = 5 with default parameters and we compared the cross-validation errors to find the most likely K. We combined the results from the different runs using the CLUMPAK server³³ with default settings.

The initial dataset was complemented with 39 additional samples that were also typed using a genotyping-by-sequencing approach but utilizing the restriction enzyme NsiI, which is an isoschizomer of EcoT22I, and using an Illumina NovaSeq 2x150 bp sequencing at the University of Wisconsin-Madison Biotechnology Center. We optimized the filtering parameters, mainly the maximum proportion of missing data, to obtain a subset of SNPs that produced genotypes consistent with those obtained when analyzing the original dataset, which were used to genotype the new individuals. We used this smaller set of markers to increase sample size for the distribution of the karyotype variants.

Whole genome sequencing

To better characterize the chromosomal limits of the inversion, we sequenced the complete genome of 16 homokaryotype males at a coverage of about 10x. We selected 10 homokaryotypes from the southwestern type (BB) from separate locations on the continent and Atlantic islands, and 6 from northern and eastern quails (AA; Table S2). DNA was extracted by phenol chloroform followed by an

ethanol precipitation. Whole genome sequencing libraries were constructed following standard protocols,⁶³ and sequenced at the SNP&SEQ Technology Platform in Uppsala (Sweden) using Illumina HiSeqX (2x150bp).

Immunofluorescence assays

Spermatocyte nuclei surface spread

To obtain spread nuclear chromatin, we performed surface spreading of spermatocyte nuclei on glass slides from frozen quail testis.⁶⁴ Briefly, a small portion of frozen tissue was minced in cold PBS to obtain cell suspensions, cells were then treated with 1% lypsol for 40 min, fixed with fresh 1% paraformaldehyde containing 0.15% Triton X-100 for 2h in a humid chamber, air-dried and washed with 0.4% Photo-Flo.

Immunofluorescence staining

To identify the chromosomes, surface spreads were stained against the axial core marker, SYCP3, using a previously described method:⁶⁵ slides were blocked for 15 min with blocking buffer (0.2% BSA, 0.2% gelatin, 0.05% Tween-20 in PBS) and then incubated with primary antibody anti-rabbit SYCP3 (1:400, Abcam Cat# ab15093, RRID:AB_301639), overnight at 4°C; after washes, slides were incubated with a goat anti-rabbit DyLight 649 (1:400, Jackson ImmunoResearch Lab Cat# 108-495-003, RRID:AB_2337515) for 1 h at 37°C. Finally, slides were mounted with Vectashield mounting medium containing DAPI. Slides were examined on a Zeiss Axioptofluorescence microscope. We captured 20–40 well-spread pachytene spermatocyte cells from each slide and saved their locations on each slide.

Fluorescence in situ hybridization (FISH) assay

Using the Japanese quail genome (*C. japonica*) as a reference (GENBANK ID GCA_001577835.1) and probes developed for chicken,⁶⁶ we synthesized probes for FISH assays. One of the probes, K19 (NCBI code WAG-22K19), was designed to hybridize to a DNA sequence inside the divergent region of chromosome 1 and the other one was outside this region (J23: WAG-22J23). Probes were labeled by nick-translation with digoxigenin-11-dUTP (Roche, for probe K19) or biotin-16-dUTP (Roche, J23). We performed an adapted FISH assay to detect the locations of the two probes on spermatocyte chromosomes.⁶⁷

Slides were denatured in 70% formamide in 2% SSC for 20 min at 77°C, incubated with 1M sodium thiocyanate for 3h, denatured again with denaturation solution for 20 min at 77°C, and dehydrated in a series of ethanol solutions. At the same time, 200–400ng DIG or Biotin-labeled probes were precipitated with Cot-1 DNA (Invitrogen) and salmon sperm DNA (Stratagene). The precipitated probe DNAs were resuspended in hybridization buffer (50% formamide, 2X SSC, and 10% dextran sulfate) under constant agitation at 37°C, denatured for 10min at 79°C, and reannealed for at least 30min at 37°C. Finally, reannealed probe DNAs were incubated on denatured slides for 72h at 37°C. After hybridization, slides were washed with 50% formamide, 2 × SSC at 45°C, rinsed with 4 × SSC containing 0.1% Tween 20, and blocked with blocking buffer (4 × SSC, 4mg/ml BSA, 0.1% Tween20) for 30min at 37°C; finally, slides were incubated with Alexa Fluor 555 streptavidin (Invitrogen, 1:100) and Anti-Digoxigenin-Fluorescein (Roche, 1:10) for 1h at 37°C, washed and air-dried.

Since SYCP3 signals were lost during the FISH assay, a second round of immunostaining against SYCP3 was performed after FISH. Then both probe and SYCP3 signals were examined and captured in pre-selected pachytene spermatocyte cells. Slides were examined using a Zeiss Axioskop epifluorescence microscope equipped with a Point Gray Research camera controlled by the ACO XY Software (A.COLOMA Open microscopy). Images were processed by Adobe Photoshop to match the intensity observed under the microscope. Measurement of distances between probes was performed using ImageJ.⁴¹

Stable isotope analyses

We washed the feathers with absolute ethanol, rinsed them with distilled water and put them in a stove to dry. We cut into small pieces two portions (0.3 mg each approximately) of the apical end of the feathers, and placed them into silver capsules for the $\delta^2\text{H}$ analyses and into tin capsules for the $\delta^{13}\text{C}$ analyses.

$\delta^2\text{H}$ quantification

Isotope measurements were performed on H^2 derived from high-temperature flash pyrolysis at 1450°C by means of Flash HT Plus elemental analyzer coupled to a Delta-V Advantage isotope ratio mass spectrometer via a CONFLO IV interface (Thermo Fisher Scientific, Bremen, Germany). Stable isotope ratio was expressed in the standard δ -notation (‰) relative to the Vienna Standard Mean Ocean Water (VSMOW). Based on laboratory standards, the measurement error was $\pm 3\text{‰}$. The standards used were: CBS, KHS, USGS-42 (keratin standards supplied by Environment Canada) and LIE-PA2 (feathers of Razorbill, internal standard). The $\delta^2\text{H}$ analyses were carried out using the comparative equilibration approach described in Wassenaar and Hobson,⁶⁸ and by using calibrated keratin isotope reference materials to avoid effects of H exchange with ambient water vapor.

$\delta^{13}\text{C}$ quantification

Samples were combusted at 1020°C using a continuous flow isotope-ratio mass spectrometry system by means of Flash HT Plus elemental analyzer coupled to a Delta-V Advantage isotope ratio mass spectrometer via a CONFLO IV interface (Thermo Fisher Scientific, Bremen, Germany). Stable isotope ratios were expressed in the standard δ -notation (‰) relative to Vienna Pee Dee Belemnite. Based on laboratory standards, the measurement error was $\pm 0.1\text{‰}$. The standards used were: EBD-23 (cow horn, internal standard), LIE-BB (whale baleen, internal standard) and LIE-PA (feathers of Razorbill, internal standard). These laboratory standards were previously calibrated with international standards supplied by the International Atomic Energy Agency (IAEA, Vienna).

QUANTIFICATION AND STATISTICAL ANALYSIS

Phenotypic data

We calculated a modified Holynski Index^{13,69,70} to measure wing pointedness based on the lengths of the primary feathers, the second secondary feather and the folded wing:

$$\text{Modified Holynski Index} = \frac{\sum \text{Prox} - \sum \text{Dist}}{\text{Wing}} * 100$$

Being:

$$\sum \text{Prox} = \sum_{i=1}^y (P_m - \text{Prox}P_{m-i}) + (P_m - S_2)$$

$$\sum \text{Dist} = \sum_{j=1}^z (P_m - \text{Dist}P_{m+j})$$

P_m : length of the largest primary feather (m)

y : number of primaries proximal to m

z : number of primaries distal to m

$\text{Prox}P_{m-i}$: length of the i^{th} proximal primary feather in relation to m

$\text{Dist}P_{m+j}$: length of the j^{th} distal primary feather in relation to m

S_2 : length of the second secondary feather

Wing : length of the folded wing

We statistically compared weight, the width of the lipid band and the modified Holynski Index among karyotype groups (AA, AB and BB) in one year old males (Euring 5) by fitting a linear model for each one of the response variables studied. Karyotype group was the explanatory variable in the three models. Homoscedasticity and normality of residuals were checked by visual exam of scatterplots (both were fulfilled). Significance was evaluated with an F -test with the function `Anova()` available in the R car package.⁷¹ Pairwise comparisons between genomic clusters were done with Tukey's posthoc tests using the function `emmeans()` from the `emmeans` package.³⁵

Throat pigmentation was categorized into six levels, from pale (level 1) to completely pigmented (level 6, Figure S5), by visual examination of throat pictures of one year old males (Euring 5) and comparing to a pre-defined scale. In any case, to avoid subjective appreciation, the characterization of quails was always done by the same researchers (JDR-T and MP) that have been working together in the study of quails for decades. We performed a Kruskal-Wallis test to test the significance of the differences in throat pigmentation among groups using the function `kruskal.test()`, and used Wilcoxon-Mann-Whitney tests to assess pairwise differences between karyotype groups with the function `wilcox.test()`. Statistical analyses were done in RStudio.

Genomic data

SNP calling and filtering

We checked sequencing data quality by using FASTQC v.0.11.5³⁶ and we removed adaptor sequences and quality trimmed with CUTADAPT v.1.17.³⁴ We mapped reads against the Japanese quail genome (RefSeq assembly accession number: GCF_001577835.2) using BWA-MEM v.0.7.15³² and we performed read group tagging and duplicate marking with PICARD v.2.4.1 (<https://broadinstitute.github.io/picard/>). We used GATK v3.6³⁸ for joint indel realignments. We used the depth option implemented in SAMtools v. 1.6.0⁵⁰ to calculate the mean depth of coverage.

We called variants across the 16 genomes using FREEBAYES v. 1.3.1,³⁷ with the flags “-X” and “-u” to ignore complex events and multi-nucleotide polymorphisms. Variants were filtered from the initial variant call set via hard-quality filters in `vcffilter` (from `vcflib`) as follows: mapping quality across samples higher than 40, additional contribution of each observation at least 10 log units, reads on both strands and at least two reads balanced to each side of the site. To remove false variants, we excluded sites with quality score smaller than two times the depth when the depth was greater than the mean depth plus the squared root of the mean depth using VCFTOOLS v.0.1.15.⁷² Afterward, we removed loci with a mean depth higher than 3 times the mean depth and those in repetitive regions, based on the soft-masked Japanese quail genome. We kept only biallelic variants located on assembled chromosomes and with less than 50% missing data and minor allele count greater than 2. After applying quality and depth filters, we kept 17,836,922 biallelic SNPs.

Population structure and differentiation

We assessed population structure with a principal component analysis (PCA) using PLINK v1.90b6.10⁴⁴ and with ADMIXTURE and CLUMPAK. These analyses were performed with SPNs from whole-genome sequences, from the inverted region in chromosome 1 and also excluding the inverted region.

After confirming the existence of a chromosomal inversion using immunofluorescence, in order to better identify the region of high differentiation, we calculated average F_{ST} between homokaryotype individuals (AA versus BB) across non overlapping 1 Kbp and 1,000 Kbp windows using the F_{ST} implemented in VCFTOOLS. We plotted F_{ST} values along the genome with the package `ggplot2`⁴⁶

in RStudio. To confirm the suppression of recombination in the inverted region, we thinned the SNP dataset for sites at a minimum distance of 10 Kbp and we calculated R^2 values in chromosome 1 with the LDHeatMap package⁴² in R for all samples and only for inverted and non-inverted samples.

The putative position of the breakpoints was estimated from the location of the transition in F_{ST} values in the inverted region of chromosome 1. However, we considered the physical location to be slightly within the divergent region and not to correspond exactly with the position of the outlier SNPs, as the increased divergence can extend beyond the breakpoints due to genetic hitchhiking. To determine the position of the breakpoints, we visually checked the read mappings around the expected position of breakpoints with IGV v.2.5.2^{39,40} to identify differential patterns of pair orientations compatible with the presence of an inversion between inverted and non-inverted samples. We carried out pairwise alignments between regions including the putative location of breakpoints using the MAFFT aligner⁴³ (<https://mafft.cbrc.jp/alignment/server/>). The visual inspection of the read mapping and the pairwise alignments did not show clear breakpoints around the region of the transition of F_{ST} . This could be due to the use of a reference genome belonging to a different species or to the absence of the breakpoint region in the reference genome. These analyses suggested that the breakpoints could be located around positions 52,100,000 and 168,610,000 on chromosome 1.

Based on a literature search, we identified 5 genes located in the inverted region that could be potential candidate for pigmentation: TYR, RAB-38, OCA2, DCT and GPR143,^{11,73–78} and one related to migratory behavior or restlessness: NPAS2.^{79–81} To assess if the gene function could be different in quails with and without the inversion, we annotated the SNP dataset with SnpEff v.4.3t⁵¹ using the GTF annotation file from the Japanese quail genome. We identified nonsynonymous mutations from the annotated SNP set to check if the gene function could have been affected by the inversion and we found one fixed non synonymous change between inverted and non-inverted chromosomal regions in RAB-38 and other three in TYR (Table S3).

Time of divergence of the sequences in the inversion

We estimated absolute divergence (d_{XY}) between the inverted and non-inverted haplotypes, which is a measure of the fraction of nucleotide differences between the two sequences, using a custom perl script (https://github.com/MattChristmas/Quail_inversion_scripts). As divergence is not consistent across the entire length of the inversion, being highest at the ends and decreasing in the middle likely due to double crossover and gene conversion events, we estimated d_{XY} for the first and last 2 Mbp of the inversion. This gave us the best estimate of accumulated divergence since the origin of the inversion event. We then converted this divergence estimate to an estimate of divergence time using the equation:

$$T = d_{XY} / (2 * \mu)$$

Where T is the divergence time in generations and μ is the mutation rate in mutations per site per generation. The mutation rate has not been estimated for the common quail so we estimated a range for T using published mutation rates for other bird species, including the ancestral bird lineage (1.23×10^{-9} site⁻¹ generation⁻¹), chicken (1.91×10^{-9} site⁻¹ generation⁻¹), zebra finch (2.21×10^{-9} site⁻¹ generation⁻¹) from Nam et al.⁸² and collared flycatcher (4.6×10^{-9} site⁻¹ generation⁻¹) from Smeds et al.⁸³ With a generation time of ~ 1 year,⁸⁴ the value of T is directly translatable to an estimate of the number of years of divergence.

Stable isotope data

We calculated the difference between the isotopic value of the primary feather grown during the previous breeding season minus the one of the primary feather grown during the last wintering season for each isotope. We fitted two linear models (one per isotope) to test whether the differences observed among genetic groups (fixed factor) were statistically significant. Homoscedasticity and normality of residuals were checked by visual exam of scatterplots (both were fulfilled). Pairwise comparisons between genomic clusters were done with the Tukey's posthoc test using the function `emmeans()` from the `emmeans` package.